

# Rectifier Neural Network with a Dual-Pathway Architecture for Image Denoising

Keting Zhang and Liqing Zhang

**Abstract**—Recently deep neural networks based on tanh activation function have shown their impressive power in image denoising. However, much training time is needed because of their very large size. In this letter, we propose a dual-pathway rectifier neural network by combining two rectifier neurons with reversed input and output weights in the same hidden layer. We drive the equivalent activation function and illustrate that it improves the efficiency of capturing information from the noisy data. The experimental results show that our model outperforms other activation functions and achieves state-of-the-art denoising performance, while the network size and the training time are significantly reduced.

**Index Terms**—deep neural network, rectifier activation function, dual-pathway architecture, image denoising.

## I. INTRODUCTION

**T**HE target of image denoising is to recover the original clean image under the additive white Gaussian noise corruption. Many effective patch-based algorithms and their variants have been proposed, such as sparse redundant representation model [1]–[3], non-local statistics model [4]–[6] and neural network model [7]–[9]. Recently the machine learning approach based on deep neural network for image denoising has draw considerable attention. This approach utilizes the strong ability of deep neural network to approximate a denoising function from a noisy patch to a clean patch. It has been shown that a multi-layer enormous plain neural network trained on a large training set is able to compete with BM3D [4] and achieves state-of-the-art denoising performance [7].

However, training such deep neural networks is very time-consuming because of their large model size. For example, as mentioned in paper [7], about one month of computation time on a GPU is required for training the proposed neural network with four hidden layers of size 2047 and both input and output layers of size 289. It was also shown that larger patch and wider hidden layers are beneficial to the denoising performance [7], [10]. Thus, long training time limits the use of deep neural network based methods in practice. In this letter, we address this problem and try to reduce the network size and the training time to make this approach more practical.

According to the analysis in [7], the trained neural network relies on the dictionary learned in the output layer to reconstruct the denoised patches. Whereas, in the context of deep

neural networks, recent emerging work has shown that rectifier activation function is more suitable for sparse data such as natural images than the traditional tanh function and performs better on many image-related tasks [11], [12]. Therefore here we try to use rectifier activation function instead of tanh for image denoising.

Furthermore, as pointed out in [11], rectifier is an one-sided function which means its response to the opposite of a strongly excitatory input is zero. We empirically analyze the dictionary learned by rectifier neurons in single hidden layer neural network and show that they tend to learn the reversed atoms due to the one-sided property. That means two individual rectifier neurons will be needed to encode the responses to two opposite excitatory patterns, respectively. Thus the efficiency of capturing information from the input data is weakened.

Inspired by this, we propose a dual-pathway architecture by combining two rectifier neurons with reversed input and output weights. This polarity coupling strategy results in an equivalent antisymmetric activation function which enables one node to respond to patterns with opposite polarities simultaneously. We empirically demonstrate that the reversed atoms are prevented by our model. Then we evaluate the deep dual-pathway rectifier neural network for image denoising. The experimental results show that our model outperforms both plain rectifier and tanh networks and achieves comparable performance to BM3D, while the network size and the training time are significantly reduced. We provide a Matlab toolbox with the trained models to test our approach.

## II. DUAL-PATHWAY RECTIFIER NEURAL NETWORK

### A. Motivation

First we examine qualitatively the effect of rectifier's one-sided property on the learned dictionary in a single hidden layer network (also known as denoising autoencoder in deep learning community). The network takes a corrupted version  $\tilde{x}$  of original clean patch  $x$  as input and maps it to a denoised patch  $y$  by:

$$y = r(\tilde{x}) = W_2 f(W_1 \tilde{x} + b_1) + b_2 \quad (1)$$

where  $W_1$  and  $W_2$  are weight matrices,  $b_1$  and  $b_2$  are bias vectors, and  $f = \max(0, x)$  is the rectifier activation function. To illustrate the learned dictionary better, we constrain  $W_1$  and  $W_2$  to be transposes of each other, i.e.,  $W_2 = W_1^T$ .

For training data, we randomly extract some natural image patches of size  $10 \times 10$  and corrupt them using additive white Gaussian noise with  $\sigma = 25$  to form the corresponding noisy patches. To eliminate the effect of the DC component, all

This work was supported by the Key Basic Research Program of Shanghai under Grant 15JC1400103 and the National Natural Science Foundation of China under Grants 91420302 and 61272251.

The authors are with Key Laboratory of Shanghai Education Commission for Intelligent Interaction and Cognitive Engineering, Department of Computer Science and Engineering, Shanghai Jiao Tong University, Shanghai, 200240 (e-mail: zzsnaill@sjtu.edu.cn; zhang-lq@cs.sjtu.edu.cn)

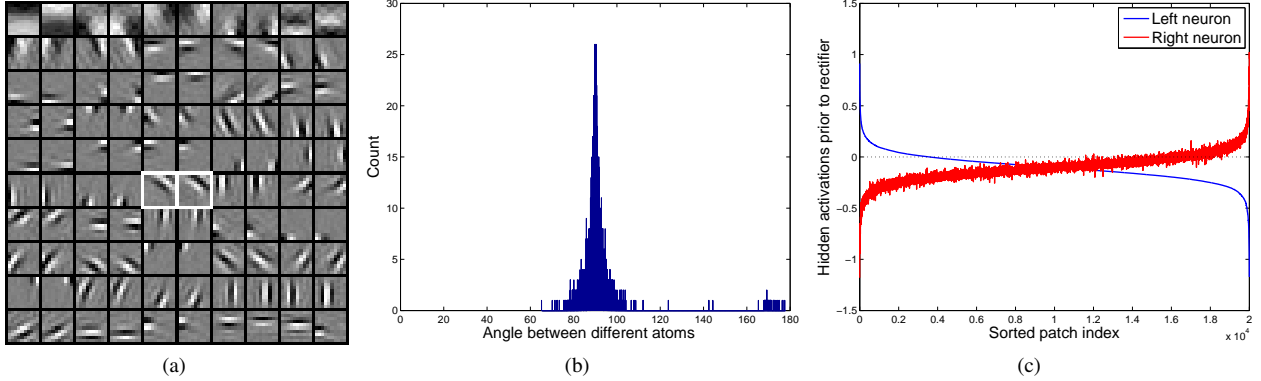


Fig. 1. The effect of one-sided property on the dictionary learned by rectifier neural network. (a) all learned atoms are shown in pairs and sorted according to the angles between atoms in each pair in descending order from left to right and from top to bottom. (b) histogram of angles between different atoms. (c) hidden activations prior to rectifier nonlinearity of two neurons corresponding to the atoms in white boxes in (a). All test patches are sorted by the activations of neuron with the left atom.

patches are preprocessed by subtracting the mean-value for each sample. We use a network with 100 hidden units to learn a dictionary consisting of 100 atoms.

The learned dictionary is shown in Fig. 1(a) in the following way. First, we compute the angles between different atoms and select two atoms with the biggest angle and display them. Then we repeat this operation on the remaining atoms and show the atoms with the second biggest angle. We continue until all atoms are displayed in a descending order. We can see that almost all pairs show opposite patterns at the same spatial location except the last two. The histogram of all angles between different atoms is plotted in Fig. 1(b), which shows that most angles are around 90 degrees, while a few are relatively large. These relatively large angles exactly correspond the first 48 atom pairs in (a), ranging from about 177 to 165 degrees. It is indicated that the atoms in different pairs are quite orthogonal to each other, while atoms in the same pair show reversed polarities.

We randomly sample some test patches and feed them into the model to observe the responses of hidden neurons. The hidden activations prior to rectifier nonlinearity of two neurons corresponding to the atoms in white boxes in (a) are shown in Fig. 1(c). The activations of right neuron fluctuate because these two atoms are not exactly opposite to each other. This figure clearly shows that many opposite patterns exist in natural images, while the rectifier neuron which can be activated by some pattern does not respond to the corresponding opposite pattern because of its one-sided property. Thus for rectifier neurons, some redundancies exist in the learned dictionary and the ability to capture information from the input is weakened. Next we will propose a dual-pathway architecture to improve it.

### B. Model Description

The basic idea of our model is that for every rectifier neuron in hidden layers, we add an extra companion node and associate it with the opposite input and output weights. Specifically, for every rectifier node connected with input weight  $w_{in}$  and output weight  $w_{out}$ , we generate a companion

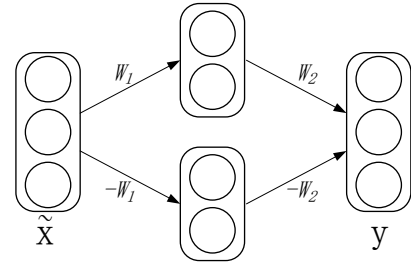


Fig. 2. Architecture of dual-pathway rectifier neural network with single hidden layer. For every neuron in hidden layer, there is an extra companion node with opposite input and output weights. The lower hidden nodes can be seen as the companions of the upper ones.

node in the same layer with input weight  $-w_{in}$  and output weight  $-w_{out}$ . By this polarity coupling strategy, later we will show that these two neurons are equivalent to one neuron with a novel activation function. The purpose of associating with  $w_{in}$  and  $-w_{in}$  is to enable the equivalent neuron to respond to both opposite patterns in data, while  $w_{out}$  and  $-w_{out}$  is to reflect the polarity of input patterns correctly.

A single hidden layer network with such architecture is shown in Fig. 2. The mapping defined by it is:

$$y = [W_2 \quad -W_2] f \left( \begin{bmatrix} W_1 \\ -W_1 \end{bmatrix} \tilde{x} + \begin{bmatrix} b_1 \\ b'_1 \end{bmatrix} \right) + b_2 \quad (2)$$

where  $\tilde{x}$  is the noisy patch,  $y$  is the obtained denoised patch, the weight matrices  $W_1$ ,  $W_2$  and biases  $b_1$ ,  $b'_1$ ,  $b_2$  are the parameters,  $f$  is rectifier function  $\max(0, x)$ .

We define a novel activation function  $g(x)$  with parameter  $t$  as follows:

$$g(x) = \max(0, x + t) - \max(0, -x + t) \quad (3)$$

Hence, if we set  $t = (b_1 + b'_1)/2$ , then

$$\begin{aligned} y &= W_2 [f(W_1 \tilde{x} + b_1) - f(-W_1 \tilde{x} + b'_1)] + b_2 \\ &= W_2 g \left( W_1 \tilde{x} + \frac{b_1 - b'_1}{2} \right) + b_2 \end{aligned} \quad (4)$$

Thus we can see that the dual-pathway architecture is equivalent to the antisymmetric activation function  $g(x)$  with train-

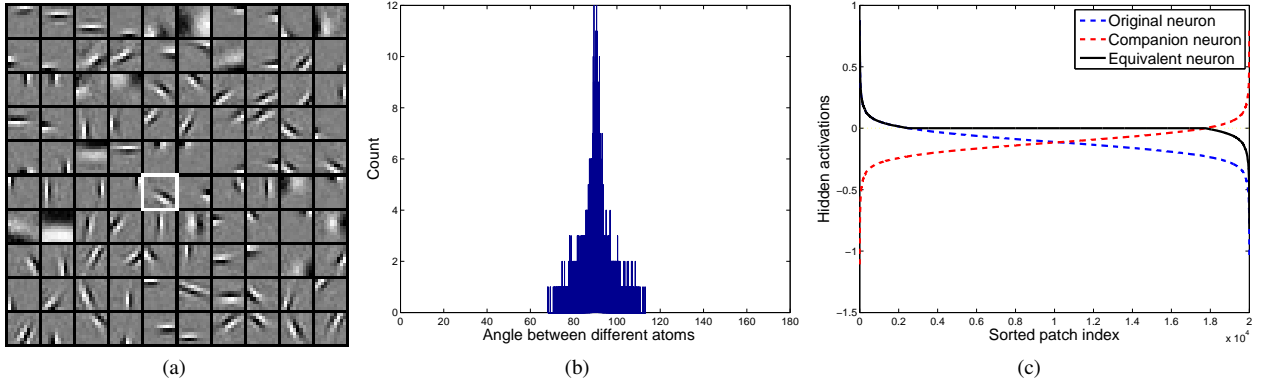


Fig. 4. Dictionary learned by a dual-pathway rectifier neural network. (a) all learned atoms are shown in the same way as Fig. 1(a). (b) histogram of angles between different atoms. (c) hidden activations prior to rectifier of original neuron (corresponding to the atom in white box in (a)) and the corresponding companion neuron, and hidden activations after rectifier of the equivalent neuron. All test patches are sorted by the activations of original neuron in descending order.

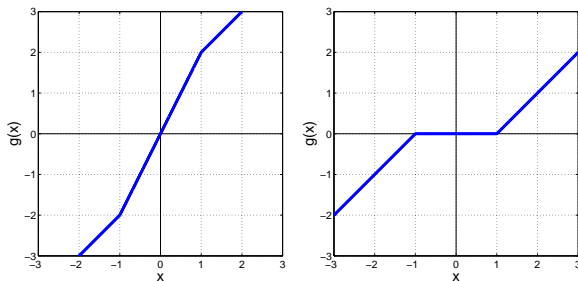


Fig. 3. Activation function  $g(x)$  with trainable parameter  $t$ . **Left:**  $t$  is non-negative ( $t = 1$ ). **Right:**  $t$  is negative ( $t = -1$ ).

able parameter  $t$ . Its shapes with non-negative and negative parameters are shown in Fig. 3.

For every hidden layer node, the activation function  $g(x)$  introduces one extra parameter  $t$  which can be learned simultaneously with weights and biases. In this paper, all network parameters are optimized using minibatch Limited memory BFGS (L-BFGS) method which is very suitable for training deep models [13]. We use L-BFGS implementation in minFunc by Mark Schmidt<sup>1</sup>.

### III. EXPERIMENTAL STUDY

In this section we discuss the empirical evaluation of our model. First we study the effect of dual-pathway architecture on dictionary learning and patch restoration. Then we apply deep dual-pathway rectifier network to image denoising.

#### A. Dictionary Learning and Patch Restoration

We carry out the similar experiment to the one in Section II-A to illustrate the effect of proposed dual-pathway model on dictionary learning. As shown in Fig. 4(a), we try to display all learned atoms in the same way as Fig. 1(a). However, we can see that none of atom pairs exhibit opposite patterns at the same spatial location, which is very different from the

plain rectifier model. Notice that although the atoms in some pairs look like each other, their locations are different. Fig. 4(b) presents the histogram of all angles between different atoms, which demonstrates that all atoms are quite orthogonal to each other. The atoms with relatively big angles close to 180 degrees do not exist.

Then we randomly choose a neuron (corresponding to the atom in the white box in Fig. 4(a)) and depict its hidden activations in Fig. 4(c). We plot the activations prior to rectifier nonlinearity of original neuron and its companion neuron using dashed lines. We can see that they detect the opposite patterns in input respectively, which is similar to plain rectifier network. Whereas the equivalent neuron combines their functions and yields responses according to the polarities of the input. This mechanism enables one single neuron to encode both opposite patterns simultaneously. The results of this comparative experiment suggest that dual-pathway architecture promote the efficiency of information capturing from the input and hence may help recovering the noisy data compared to single-pathway network.

To evaluate the effect of dual-pathway architecture on patch restoration, we compute the root mean square error (RMSE) averaged on 20000 test patches of both models. We vary the overcompleteness ratio from  $1 \times$  to  $8 \times$  to observe the impact of dictionary scales on the performance gains. Thus the number of dictionary atoms ranges from 100 to 800. As shown in Fig. 5, we can see that the proposed dual-pathway architecture indeed provides greater efficiency of extracting information and yields lower reconstruction error as expected, although the improvement decreases as the dictionary scale increases.

#### B. Natural Image Denoising

Following the protocol in [7], given a noisy image, we first chop it into a number of overlapping noisy patches. Then we apply our trained network model to them and get the denoised versions. Finally, all denoised patches are put at the positions of their noisy counterparts and aggregated on the overlapping regions via Gaussian weighted averaging.

Different from [7], we adopt a small deep network architecture with four hidden layers of size 512, an input layer

<sup>1</sup><http://www.cs.ubc.ca/~schmidtm/Software/minFunc.html>

TABLE I

COMPARISONS OF THE DENOISING PERFORMANCES OF FOUR MODELS MEASURED BY PSNR. TOP LEFT: BM3D METHOD [4]. TOP RIGHT: PLAIN TANH NETWORK. BOTTOM LEFT: PLAIN RECTIFIER NETWORK. BOTTOM RIGHT: DUAL-PATHWAY RECTIFIER NETWORK. THE LAST ROW REPRESENTS THE AVERAGE RESULTS OVER ALL IMAGES.

$\sigma$ /PSNR	15/24.61		25/20.17		35/17.25		50/14.15		75/10.63		100/8.13	
Cameraman	<b>31.85</b>	31.15	29.44	28.98	<b>27.98</b>	27.58	26.10	26.05	24.27	24.11	<b>22.97</b>	22.65
	31.45	31.80	29.22	<b>29.47</b>	27.71	27.95	26.03	<b>26.30</b>	23.90	<b>24.29</b>	22.41	22.76
Boat	<b>32.07</b>	31.64	29.81	29.60	28.32	28.23	26.68	26.82	25.01	25.21	23.89	24.03
	31.87	32.06	29.75	<b>29.85</b>	28.31	<b>28.41</b>	26.81	<b>26.91</b>	25.18	<b>25.26</b>	24.03	<b>24.06</b>
Bridge	28.78	28.79	26.23	26.41	24.86	25.01	23.57	<b>23.70</b>	22.38	<b>22.45</b>	21.59	21.60
	28.85	<b>28.87</b>	<b>26.44</b>	26.41	25.01	24.97	23.66	23.66	22.37	22.42	21.57	<b>21.62</b>
Couple	<b>32.10</b>	31.60	<b>29.69</b>	29.37	28.09	27.91	26.42	26.39	<b>24.69</b>	24.64	23.52	23.48
	31.83	32.01	29.56	29.66	28.06	<b>28.11</b>	26.42	<b>26.46</b>	24.58	24.67	23.47	<b>23.54</b>
Hill	<b>31.86</b>	31.59	<b>29.79</b>	29.61	<b>28.47</b>	28.35	27.08	27.08	25.57	25.61	24.50	24.52
	31.69	31.84	29.68	29.78	28.39	28.46	27.08	<b>27.12</b>	25.61	<b>25.63</b>	<b>24.61</b>	24.60
Lena	<b>34.24</b>	33.71	<b>32.06</b>	31.75	30.54	30.37	<b>28.95</b>	28.80	<b>27.09</b>	26.98	<b>25.70</b>	25.61
	34.02	34.16	31.97	31.99	30.53	<b>30.55</b>	28.87	28.88	26.99	27.01	25.68	25.69
Man	31.92	31.71	29.59	29.57	28.22	28.25	26.81	26.92	25.31	25.39	24.21	24.26
	31.90	<b>32.04</b>	29.69	<b>29.75</b>	28.31	<b>28.35</b>	26.92	<b>26.98</b>	25.37	25.39	24.28	<b>24.31</b>
Peppers	32.74	32.16	30.24	29.94	28.62	28.41	26.79	26.64	24.86	24.50	<b>23.39</b>	22.94
	32.43	<b>32.75</b>	30.13	<b>30.34</b>	28.60	<b>28.77</b>	26.74	<b>26.91</b>	24.59	<b>24.87</b>	22.92	23.22
Average	<b>31.95</b>	31.54	29.61	29.40	28.14	28.01	26.55	26.55	24.90	24.86	23.72	23.64
	31.76	31.94	29.56	<b>29.66</b>	28.12	<b>28.20</b>	26.57	<b>26.65</b>	24.82	<b>24.94</b>	23.62	<b>23.73</b>

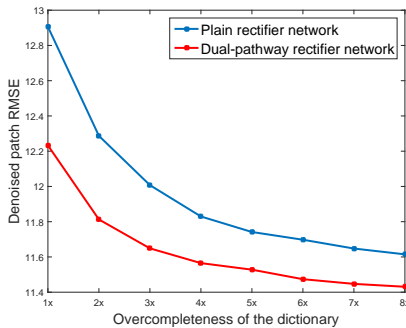


Fig. 5. Denoised patch RMSE with  $\sigma = 25$  obtained by plain and dual-pathway rectifier networks with single hidden layer of different scales.

of size 289 and an output layer of size 81. This network takes a  $17 \times 17$  noisy patch as input and tries to recover its central  $9 \times 9$  block as output. The number of dictionary atoms learned by the output layer is 512, which is about 6 times as large as the denoised patch size. We use the natural images in the Berkeley segmentation database [14] and convert them to gray-scale images to generate the training patches. Six levels of additive white Gaussian noise with standard deviations 15, 25, 35, 50, 75 and 100 are tested. For every specific noise level, we generate 50 million training samples and choose the minibatch size 10000. The training of the model requires about 2 days of computation time on single Tesla K20c GPU.

We compare the proposed dual-pathway rectifier network with plain tanh and rectifier networks of identical architecture, and BM3D method. Quantitative comparisons over eight

standard test images are performed using the Peak Signal to Noise Ratio (PSNR):  $10 \log_{10}(255^2/\sigma_e^2)$ , where  $\sigma_e^2$  is the mean squared error between the recovered and original images. The denoising performances of these models under all noise levels are summarized in Table I, from which we can make the following observations.

Compared to plain tanh network, our model achieves better results especially when the noise levels are low. The average improvements over tanh network are 0.4dB, 0.26dB and 0.19dB when the noise levels are 15, 25 and 35, respectively. As the noise increases, the improvements become small but there are still about 0.1dB gains. The dual-pathway architecture also outperforms plain rectifier network and the average PSNR gains range from 0.08dB to 0.18dB. This confirms the effectiveness of dual-pathway architecture in image denoising, which is consistent with the analysis in previous subsection. Thus, the proposed model or the equivalent activation function performs the best under the same network architecture. In addition, our model achieves comparable performances to the state-of-the-art BM3D method even with a small network size. The benefit is the significant reduction of training time which makes the machine learning approach based on deep neural network for image denoising more practical.

#### IV. CONCLUSION

In this paper, we have proposed a dual-pathway rectifier network for image denoising. By polarity coupling, our model improves the efficiency of dictionary learning and achieves state-of-the-art image denoising performance, while the network size and the training time are significantly reduced. For

future work we can adapt our model to other image processing problems such as image deblurring.

#### REFERENCES

- [1] M. Elad and M. Aharon, "Image denoising via sparse and redundant representations over learned dictionaries," *IEEE Trans. Image Process.*, vol. 15, no. 12, pp. 3736–3745, 2006.
- [2] S. K. Sahoo and A. Makur, "Enhancing image denoising by controlling noise incursion in learned dictionaries," *IEEE Signal Process. Lett.*, vol. 22, no. 8, pp. 1123–1126, 2015.
- [3] J. Feng, L. Song, X. Huo, X. Yang, and W. Zhang, "An optimized pixel-wise weighting approach for patch-based image denoising," *IEEE Signal Process. Lett.*, vol. 22, no. 1, pp. 115–119, 2015.
- [4] K. Dabov, A. Foi, V. Katkovnik, and K. Egiazarian, "Image denoising by sparse 3-d transform-domain collaborative filtering," *IEEE Trans. Image Process.*, vol. 16, no. 8, pp. 2080–2095, 2007.
- [5] J. Mairal, F. Bach, J. Ponce, G. Sapiro, and A. Zisserman, "Non-local sparse models for image restoration," in *Proc. IEEE Int. Conf. Computer Vision*, 2009, pp. 2272–2279.
- [6] Z. Sun and S. Chen, "Analysis of non-local euclidean medians and its improvement," *IEEE Signal Process. Lett.*, vol. 20, no. 4, pp. 303–306, 2013.
- [7] H. C. Burger, C. J. Schuler, and S. Harmeling, "Image denoising: Can plain neural networks compete with bm3d?" in *Proc. IEEE Int. Conf. Computer Vision and Pattern Recognition*, 2012, pp. 2392–2399.
- [8] Y.-Q. Wang and J.-M. Morel, "Can a single image denoising neural network handle all levels of gaussian noise?" *IEEE Signal Process. Lett.*, vol. 21, no. 9, pp. 1150–1153, 2014.
- [9] Y.-Q. Wang, "A note on the size of denoising neural networks," *SIAM J. Imag. Sci.*, vol. 9, no. 1, pp. 275–286, 2016.
- [10] H. Burger, "Modelling and learning approaches to image denoising," Ph.D. dissertation, Eberhard Karls Universität Tübingen, Tübingen, Germany, 2013.
- [11] X. Glorot, A. Bordes, and Y. Bengio, "Deep sparse rectifier neural networks," in *Proc. Int. Conf. on Artificial Intelligence and Statistics*, vol. 15, no. 106, 2011, p. 275.
- [12] A. Krizhevsky, I. Sutskever, and G. E. Hinton, "Imagenet classification with deep convolutional neural networks," in *Advances in neural information processing systems*, 2012, pp. 1097–1105.
- [13] J. Ngiam, A. Coates, A. Lahiri, B. Prochnow, Q. V. Le, and A. Y. Ng, "On optimization methods for deep learning," in *Proc. Int. Conf. on Machine Learning*, 2011, pp. 265–272.
- [14] D. Martin, C. Fowlkes, D. Tal, and J. Malik, "A database of human segmented natural images and its application to evaluating segmentation algorithms and measuring ecological statistics," in *Proc. IEEE Int. Conf. Computer Vision*, vol. 2, 2001, pp. 416–423.